



The Society shall not be responsible for statements or opinions advanced in papers or discussion at meetings of the Society or of its Divisions or Sections, or printed in its publications. Discussion is printed only if the paper is published in an ASME Journal. Authorization to photocopy material for internal or personal use under circumstance not falling within the fair use provisions of the Copyright Act is granted by ASME to libraries and other users registered with the Copyright Clearance Center (CCC) Transactional Reporting Service provided that the base fee of \$0.30 per page is paid directly to the CCC, 27 Congress Street, Salem MA 01970. Requests for special permission or bulk reproduction should be addressed to the ASME Technical Publishing Department.

Copyright © 1997 by ASME

All Rights Reserved

Printed in U.S.A

COMPUTATIONAL AND EXPERIMENTAL INVESTIGATIONS OF STRAIGHT - THROUGH LABYRINTH SEALS



B.V.S.S.S. Prasad,
Associate Professor,
I.I.T., Madras,
Chennai-600 036, India.

V. Sethu Manavalan,
Scientist-C,
Gas Turbine Research Establishment,
Bangalore-560 093, India.

N. Nanjunda Rao,
Scientist - F,
Gas Turbine Research Establishment,
Bangalore-560 093, India.

ABSTRACT

Computational and experimental investigations are carried out to estimate leakage flow rate in a static straight-through labyrinth seal. Tests were conducted over a range of pressure ratios, varying from 1.003 to 1.897, for three clearance values of 0.2, 0.36 and 0.6 mm respectively. The measured values of leakage flow parameter are corroborated with the results obtained from the simulations using FLUENT computer package. The agreement was within 8.6%. The flow details, e.g., the stream line pattern, velocity vectors, static pressure and turbulent kinetic energy in a typical seal passage, are presented.

As the flow takes place through the successive cavities of the labyrinth seal, the available pressure head of the fluid is converted to kinetic energy and then dissipated to heat by viscous shear. Whilst the quantity of the leakage flow rate is dependent on various seal parameters such as the clearance ratio, aspect ratio, pitch ratio and the number of seal teeth, the optimal design of labyrinth seal is a judicious choice of these variables. For example, the dimension of the pitch and the number of teeth lands should be so chosen to maximise the leakage resistance and minimise the kinetic energy carry-over.

On the other hand, more innovative designs with finer geometric variations in the seal configurations can be made possible only with the ability to understand the minute details of flow taking place in the passages of seal teeth. For instance, the leakage resistance can be substantially increased by a configuration that would give rise to large turbulence generation rates either upstream or downstream of the vena-contracta formed at each constriction[2].

The objective of present paper is to use a state of the art numerical code for studying the flow behaviour in a straight-through labyrinth seal. The results are sought to be corroborated by conducting experiments for the same seal configuration.

NOMENCLATURE

A	-	Labyrinth seal flow area, m ²
b	-	Seal tooth width, m
Cl	-	Radial seal clearance, m
d	-	Seal carrier outer diameter, m
h	-	Seal tooth height, m
m	-	Mass flow rate, Kg/sec.
N	-	Number of seal teeth
p	-	Pressure, Pa
Q	-	Volumetric flow rate, m ³ /sec.
S	-	Seal Pitch, m
T	-	Temperature, K
u	-	Velocity in the axial direction, m/sec.

Subscripts:

0	-	Upstream condition
1	-	Downstream condition
t	-	Turbulent quantity

BACKGROUND

The problem of establishing the leakage flow rates through labyrinth seals is fairly old. The two one-dimensional fluid dynamic approaches adopted for the problem were based on i) expansion through a series of throttling nozzles [3] and ii) pipe friction models [4]. However, a large amount of experimental data are available in the literature and the available correlations for the measured leakage flow rate through the seal are summarised in the references [3-5].

We summarised the available geometric information about straight-through labyrinth seals of various investigators [1,2 and 5-23] and presented them in the dimensionless form, refer to Table 1. The following conclusions could be drawn from the literature information:

- a) The increase in the number of seal teeth will reduce the leakage flow parameter as it leads to reduction in the kinetic energy for a given seal pressure ratio. This, however, increases the total space requirement.
- b) The smaller the seal clearance, the lower the leakage flow parameter.
- c) The lowest coefficient of discharge is obtained when the edges of the teeth have sharp corners.

INTRODUCTION

Labyrinth seals are commonly used in the secondary air system of a modern gas turbine for reducing the cooling air leakage from high pressure regions into low pressure zones, - preventing hot air ingestion from main stream into cooling air areas and for balancing the axial thrust loads at the bearings. It is well known that the performance parameters of the gas turbine such as the thermal and propulsive efficiencies and the specific fuel consumption (SFC) are strongly influenced by the leakage flow rates. According to one estimate [1], an increase of 10% cooling air leakage leads to about 0.5% increase in the SFC. Therefore any improvement in reducing the leakage flow through the seals results in the increase in the gas turbine plant efficiency.

Table 1 Summary of geometric variables for straight-through seals available in the literature

Sl. No.	Author & Year	Geometrical Parameters in mm					Geometrical Ratios						
		Seal outer dia (d)	Seal clearance (Cl)	Seal pitch (S)	Seal height (h)	Seal tooth width (b)	Cl/d	S/d	h/d	b/d	b/Cl	b/S	N
1	Kearson and Keh (1950) [5]	127	0.12065 to 0.3302	25.4	25	6.35	9.5x10 ⁻⁴ to 2.6x10 ⁻³	0.2	0.19685	0.050	52.63 to 19.23	0.25	6 to 40
2	Geza Veres (1961) [6]	254	0.1016 to 1.524	5.08	5.08	0.381	4x10 ⁻⁴	0.02	0.02	0.0015	3.75 to 0.25	0.075	3 to 34
3	Koenig (1972) [7]	269.24	0.254 to 0.508	11.43 to 9.652	15.24	0.508	9.433x10 ⁻⁴ to 1.886x10 ⁻³	0.04245 to 0.03584	0.05660	0.001886	1 to 2	0.044 to 0.0526	15
4	Mahler (1972) [8]	*	0.8382	12.7	7.62	0.3353 to 0.8382	*	*	*	*	0.3354 to 1	0.0264 to 0.066	12
5	GE, fluid flow division (1973) [9]	254	1.016	6.35	6.35	0.381	4x10 ⁻³	0.025	0.025	0.0015	0.375	0.06	5
6	Meyer (1975) [10]	200	0.127 to 2.032	127	50	0.63	6.35x10 ⁻⁴ to 0.01016	0.0635	0.25	0.00315	4.960 to 0.310	0.0496	3
7	Komatori (1977) [11]	200	0.36 to 0.46	6	2.5	6 to 1.00	1.8x10 ⁻³ to 2.3x10 ⁻³	0.03	0.0125	0.03 to 0.005	16.67 to 13.043	1	1 to 12
8	Stocker (1978) [1]	153	0.13 to 0.51	2.79	2.79	0.25	8.49x10 ⁻⁴ to 3.33x10 ⁻³	0.0182	0.0182	0.001633	1.9231 to 0.490	0.08961	4
9	Stoff (1980) [12]	955	5	50	47.5	5	5.2x10 ⁻³	0.05235	0.04973	0.0052356	1	0.1	3
10	Rhode (1986)a [13]	85.348	0.216	1.113	0.889	0.17	2.53x10 ⁻³	0.01304	0.01042	0.001992	0.7870	0.1527	2
11	Rhode (1986)b [2]	151.368	0.406	3.10	3.175	0.1524	2.68x10 ⁻³	0.02047	0.02097	0.0010068	0.3754	0.04916	16
12	Sturgess [14] (1988)	76	0.13 to 0.51	2.79	2.79	0.25	1.710x10 ⁻³ to 6.710x10 ⁻³	0.03671	0.03671	0.0032895	1.9231 to 0.4902	0.08961	4
13	Brownell (1989) [15]	10x20	0.55	5.0	4.0	0.4	0.055	0.5	0.4	0.04	0.7272	0.08	5
14	Demko (1990) [16]	772	0.635	1.635	1.905	0.635	8.225x10 ⁻⁴	2.117x10 ⁻³	0.00247	0.0008225	1	0.3883	5
15	Zhu Yizhang and He Feng (1990) [17]	*	0.5 to 2	25	4.6	*	*	*	*	*	*	*	5 to 18
16	Rhode (1992)a [18]	145	0.41	2.825	3.18	0.35	2.827x10 ⁻³	0.01948	0.02195	0.002413	0.8536	0.12389	5
17	Rhode (1992)b [19]	76	0.25	2.79	2.79	0.15 to 0.50	3.28947x10 ⁻³	0.03671	0.03671	0.001973 to 0.006578	0.6 to 2	0.05376 to 0.1792	4
18	Milward (1996) [20]	388	1.067	4.5	3.20	0.30	2.75x10 ⁻³	0.01159	0.00825	0.8247 to 0.000773	0.28116	0.0667	3
19	Sethu Manavalan (1996) [21-23, 28]	356.28	0.20 to 0.60	6	6	0.25	5.6136x10 ⁻⁴ to 1.6841x10 ⁻³	0.01684	0.01684	7.61715 x 10 ⁻⁴	1.25 to 0.04167	0.04167	3

* Data not available

- d) The coefficient of discharge increases with increasing values of tooth thickness (b) to clearance (Cl) ratio. This characteristic is attributable to the improved recovery at the vena contracta. The value of the coefficient, however, decreases for increasing values of b/Cl for porous, serrated and rough lands, e.g., honeycomb[8].
- e) An increase in the values of either the seal pitch or tooth height produces larger vortices in the seal cavities, resulting in additional pressure loss between restrictions and hence lower leakage rates. These losses, however, are small for well-designed seals. An optimum tooth height exists at a cavity aspect ratio (defined as (s-b)/h) near 0.25, see [11].

Sneck[24] in his survey paper pointed out that appropriate mix of the available theory and empirical data could predict the performance of an "ideal-labyrinth", and if the dissipation of kinetic energy is relatively incomplete, such a prediction is not possible. He concluded that until a better understanding of the dissipation process is achieved, decisions regarding sizing of the chamber depth

and width or restrictor pitch will continue to be made using rough rules of thumb or sketchy empirical evidence.

Stoff[12] is perhaps the first to model the incompressible flow in a labyrinth seal using the turbulent kinetic energy (k) - dissipation (ε) model for explaining the leakage phenomena. The influence of the turbulent fluctuations on the mean momentum transport is represented by the model. The induced secondary mean flow vortex pattern inside the cavities is favourably compared with the measurements obtained by a laser-Doppler anemometer.

Rhode et al.[13] used the TEACH programme which employs the QUICK finite differencing scheme. They found good agreement between the measured and the predicted values of leakage flow parameters. Rhode and Hibbs [19] extended the work to find out the effect of tooth thickness on the performance of the labyrinth seal. However, they found that the swirl development was only slightly higher for thicker teeth. They concluded that the leakage is almost independent of tooth thickness, although the second cavity yielded a

definite increase in the turbulent energy and length scales over the first cavity. Using the same numerical approach, Rhode and co-workers [25-27] published a series of papers testing different seal configurations.

In view of the foregoing, it is envisaged that the dependence of seal design methods on empirical practices could be reduced or eliminated if the application of a general purpose computer code were successful. It is with this objective, the present paper aims at analysing the incompressible flow in a straight-through labyrinth seal by using a Computational Fluid Dynamic package, FLUENT. Experiments on the same seal geometry were conducted and the measured values of overall leakage flow rates are corroborated with the numerical results.

EXPERIMENTS :

The experimental test facility for conducting leakage flow rate measurements in the static test seals consisted of the air supply facility, labyrinth seal test section and assembly and the necessary instrumentation. The air supply unit consisted of water cooled balanced horizontal twin compressors and an air receiver. The free air delivery of the compressor was 10.1 m³/min at a maximum pressure of 1.03 MPa. The flow to the labyrinth seal test section was controlled by a pressure regulating valve between air receiver and the test section inlet pipeline. The open circuit test loop also consisted of two more pressure control valves just at the upstream and at the downstream locations of the test section for precise control of the pressure ratio.

The labyrinth seal test rig consisted of two mild steel air inlet chambers, one at the entry seal and the other at the exit of test section, a seal carrier (consisting three straight-through seals), a support for seal drum and a plain land, Fig.1. The concentricity between the seal carrier and plain drum was ensured at the mating surfaces of the support drum and the air exit chamber at the time of assembly. The concentricity of the seal parts was ascertained in the similar fashion during the assembly of each test configuration. The possibility of leaks through the flanges and other bolted joints was prevented. The same seal drum was used for three different seal clearances by electroplating the inner surface of the drum with copper in order to minimise the manufacturing effort. After machining of the inner diameter, the seal drum was inspected for the seal clearance to ensure close tolerance. The support for the seal carrier was adjusted by locating the matching angular positions between the plain land and the seal carrier with the help of feeler gauges. The central bolt was tightened at the final assembly stage only after ensuring the uniform clearance to a tolerance of 0.01mm. Three clearances between 0.20, 0.36 and 0.60 mm were chosen for testing.

Each test data set included the measured values of upstream and down stream pressures, stagnation temperature at the upstream and the volumetric flow rate recorded by the Rockwin make turbine flow meter. The upstream and downstream static pressures were measured from ten tapping connections around the test section, recorded by a 48-channel Scanivalve and a microprocessor-printer system. The mass flow rate through the labyrinth seal was determined from the measured volume flow rate under steady operating conditions by the turbine flow meter and the density evaluated corresponding to the upstream pressure. The stagnation temperature reading was taken at the upstream of test section by a RTD thermometer and the barometer reading was noted before every test run.

A set of twelve data is taken for each clearance setting. The experiments were repeated three times for the determination of uncertainty as well as to ensure system reliability. Table 2 gives a typical test data set for the straight-through seal of 0.36 mm

clearance. The estimated experimental uncertainty is also indicated in the table.

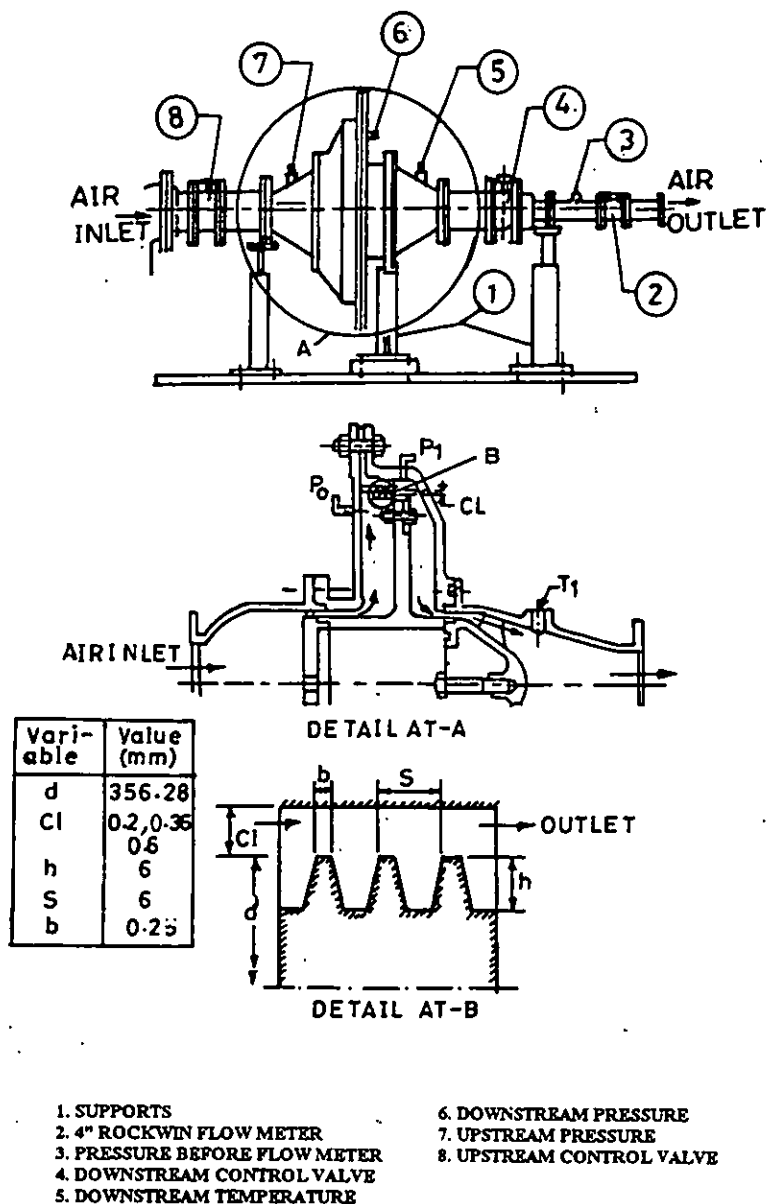


FIG. 1 SCHEMATIC DIAGRAM OF STRAIGHT-THROUGH LABYRINTH SEAL TEST RIG

Table 2 Experimental Data for a Straight-Through Labyrinth Seal, Cl = 0.36 mm.

Sl. No	Upst. Press. P ₀ (kPa)	Downst. Press. P ₁ (kPa)	Press. ratio (P ₀ /P ₁)	Mass flow rate m (kg/sec.)	Flow parameter m√T ₀ /A _{p₀}	Calculated uncertainty (%)
1	91.386	91.107	1.0031	0.005675	0.0026628	4.00
2	94.551	.293	1.0357	0.016526	0.0074912	4.20
3	100.695	92.503	1.0886	0.027303	0.0116209	4.10
4	108.793	93.806	1.1596	0.038118	0.0150180	4.76
5	118.660	95.761	1.2391	0.048392	0.0174804	4.25
6	136.252	98.181	1.3780	0.064613	0.0203260	4.38
7	149.563	101.625	1.4717	0.075427	0.0216163	4.02
8	163.432	104.976	1.5568	0.086414	0.0226642	4.87
9	179.349	110.096	1.6370	0.098391	0.0235152	4.76
10	202.155	113.540	1.7805	0.113736	0.0241160	4.02
11	218.351	117.449	1.8591	0.124596	0.0244586	4.38
12	228.497	120.428	1.8974	0.130575	0.0248945	4.90

SOLUTION PROCEDURE:

The FLUENT computer code utilises the finite volume method for discretising the governing equations and employs the body - fitted - co-ordinate system for mapping the physical plane to the computational domain. We opted for the two-equation k-ε turbulence model. The values of the modelling constants used in the package are, incidentally, identical with those obtained by Stoff [12]. They are given by:

$$C_{\mu} = 0.09; \sigma_0 = 1.00; \sigma_{\epsilon} = 1.21; C_1 = 1.44; C_2 = 1.92; C_D = 100$$

The numerical interpolation of the integrals is carried out by the power law scheme available in the package. Its main advantage has been computationally less expensive yet giving accuracies on par with the higher order schemes. Note that once the set of options of these methods are chosen, they are not changed in the entire of range of calculations. As these methods are now somewhat routinely used, no details are given for the sake of brevity. The solution of the so formulated algebraic set of equations is obtained QUICK by SIMPLE algorithm in the code. The convergence is considered to have been obtained when the sum of the residual errors for the pressure, velocity and dissipation of kinetic energy was less than 0.4, 0.3 and 0.3 percent respectively. The grid size was systematically varied from 22 x 24 to 122 x 68 to test the grid independence.

VALIDATION TESTS:

The results are generated for a "bench mark" seal configuration given in reference [14], for six grid sizes in the aforesaid range. The input data to the programme are inlet stagnation and the outlet static pressure values, apart from the fluid properties. Typically, convergence was achieved within an accuracy of 10^{-4} , in 8600 iterations for the reading no.4, Table 3.

Table 3 Comparison of computed results for a bench-mark labyrinth seal, Ref. [14]

Inlet pressure P_0 (kPa)	Exit pressure P_1 (kPa)	$m\sqrt{T_0}/A_{p_0}$ Ref. [14] (Kg-√K/N-Sec.)			Present (Kg-√K/N-Sec.)			
		Exptl. (a)	Numerl. (b)	%devn. (a)&(b)	Grid size	$m\sqrt{T_0}/A_{p_0}$ Fluent (c)	No. of Itms.	% devn. (b)&(c)
228.49	120.43	0.028462	0.030769	8.11	20X16	0.03523	3500	14.50
					40X36	0.03406	6200	10.70
					60X36	0.03310	7300	7.60
					76X36	0.03523	8600	4.53
					122X68	0.02977	1600	4.68

The agreement between the previous computations [14] and the output from the present computations is very good, as evident from Table 3; the maximum deviation in the gross leakage flow rate being 4.53%. As evident from the computational experiments at columns 6 and 9 of Table 3, the test case led to the choice of an optimal grid size of 76x36 in terms of the computational time and the accuracy. The convergence criterion for all the computations was chosen to be the accuracy of 10^{-4} .

RESULTS

The leakage flow rates, generalized in the form of the flow parameter, $m\sqrt{T_0}/A_{p_0}$, are calculated from the FLUENT code and are tabulated in Table 4, column 4. These computed values are compared with the

experimental data (Table 2, column 6) see columns 3 and 4 of Table 4. It is evident from Table 4 that the present simulation is accurate within 8.6%. However, the positive bias in the error is always higher than the experimental uncertainty. The discrepancy may, however, be attributed to an overall experimental error.

Table 4 Comparison of Computational Results with the Experiments

Sl. No.	Pr. ratio P/P ₀	Mass flow Parameter, $m\sqrt{T_0}/A_{p_0}$ (Kg-√K/N-Sec.)		Deviation +(%)
		Experimental	Computational	
1	1.0031	0.0026628	0.0027571	3.54
2	1.0357	0.0074911	0.0077616	3.61
3	1.0886	0.0116209	0.0121101	4.21
4	1.1596	0.0150183	0.0157091	4.60
5	1.2391	0.0174480	0.0183378	5.10
6	1.3780	0.0203260	0.0214642	5.60
7	1.4717	0.0216163	0.0229197	6.03
8	1.5568	0.0226642	0.0241283	6.46
9	1.6570	0.0235152	0.0251353	6.89
10	1.7805	0.0241160	0.0258547	7.21
11	1.8591	0.0244586	0.0263174	7.60
12	1.8974	0.024940	0.0244082	8.51

The plots of streamlines, velocity vectors, static pressure and kinetic energy-of turbulence contours are shown in Figs.2 to 5 for a straight-through labyrinth seal.

Fig.2 shows the streamline pattern for the flow through the seal. Recirculation regions are visible in all the cavities between the teeth. A large clockwise recirculation zone is discernible downstream of the last land. In the clearance gap, the core of the streamlines is undisturbed from the first land to the last land. However, the streamlines away from the centerline of the clearance gap are observed to be diverging and converging alternately at the exit and entrance of the seal teeth. This behaviour shows that the streamlines are subjected to the expansion and contraction process, including that at vena-contracta.

The Mach number variations are presented in Fig.3. The peak Mach number occurs near the centerline of the core region and then reduces on either side, namely, above and below the centerline. The flow from the trailing edge of the first tooth impinges on the second tooth in the vicinity of the point R, marked in Fig.3. The fluid that spread towards the bottom of the cavity, exhibits a boundary layer behaviour along all the three walls of the cavity. However, four distinct Mach number zones may be identified in the middle of the cavity: one at the bottom, two at the sides and one at the center. But at the exit of the third tooth, the flow has to meet with sudden expansion and hence the reduction of Mach number, refer to Fig.3. The velocity vector nearer to the tips of the two teeth are shown in the inset of Fig.3. The change in the shape of the vectors is due to the flow of fluid that spreads upward after impinging on the tooth and mixes with the flow in the core region.

Typical static pressure and Mach number variations, integrated across the transverse planes, are plotted along the seal in Fig.4, in addition to the constant pressure contours. Whilst the isobar patterns are similar in the cavities, the value of static pressure decreases along the seal. However, the pressure drop across the first tooth is higher (typically 0.05 MPa, Fig.4) than the second (0.021 MPa) and the third (0.029 MPa). On the other hand, the velocity (Mach number) variation along the flow path shows that the kinetic energy carried over to successive teeth is significant. These observations explain the errors found by the previous investigators, see Sneek [24], in the models based on an "ideal labyrinth", which assume (i) no kinetic energy carry-over and (ii) equal pressure drop across each seal cavity. The static pressure and the Mach number variations, together, reveal a region of pressure recovery in the cavity, for example, the maximum pressure in the first cavity arises near the point, R.

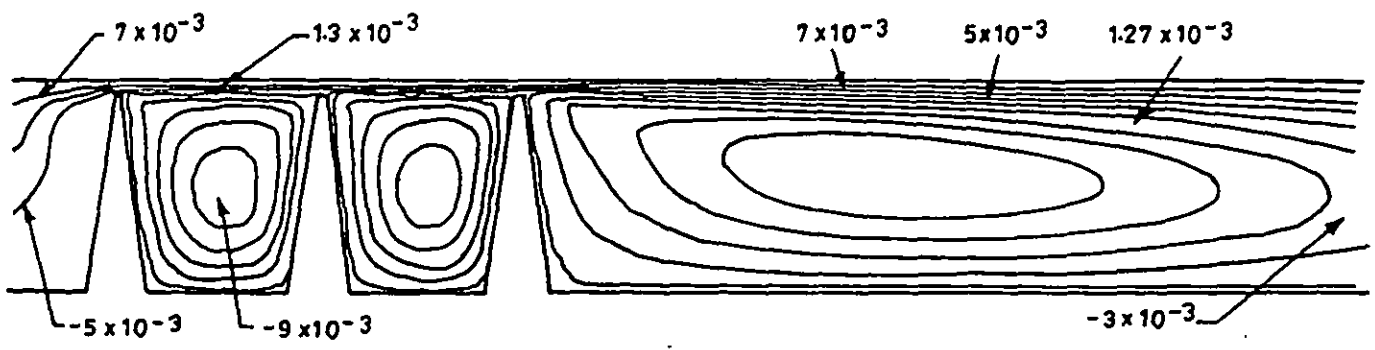


FIG. 2 STREAM LINE PATTERN ($p_0/p_1 = 1.89$)

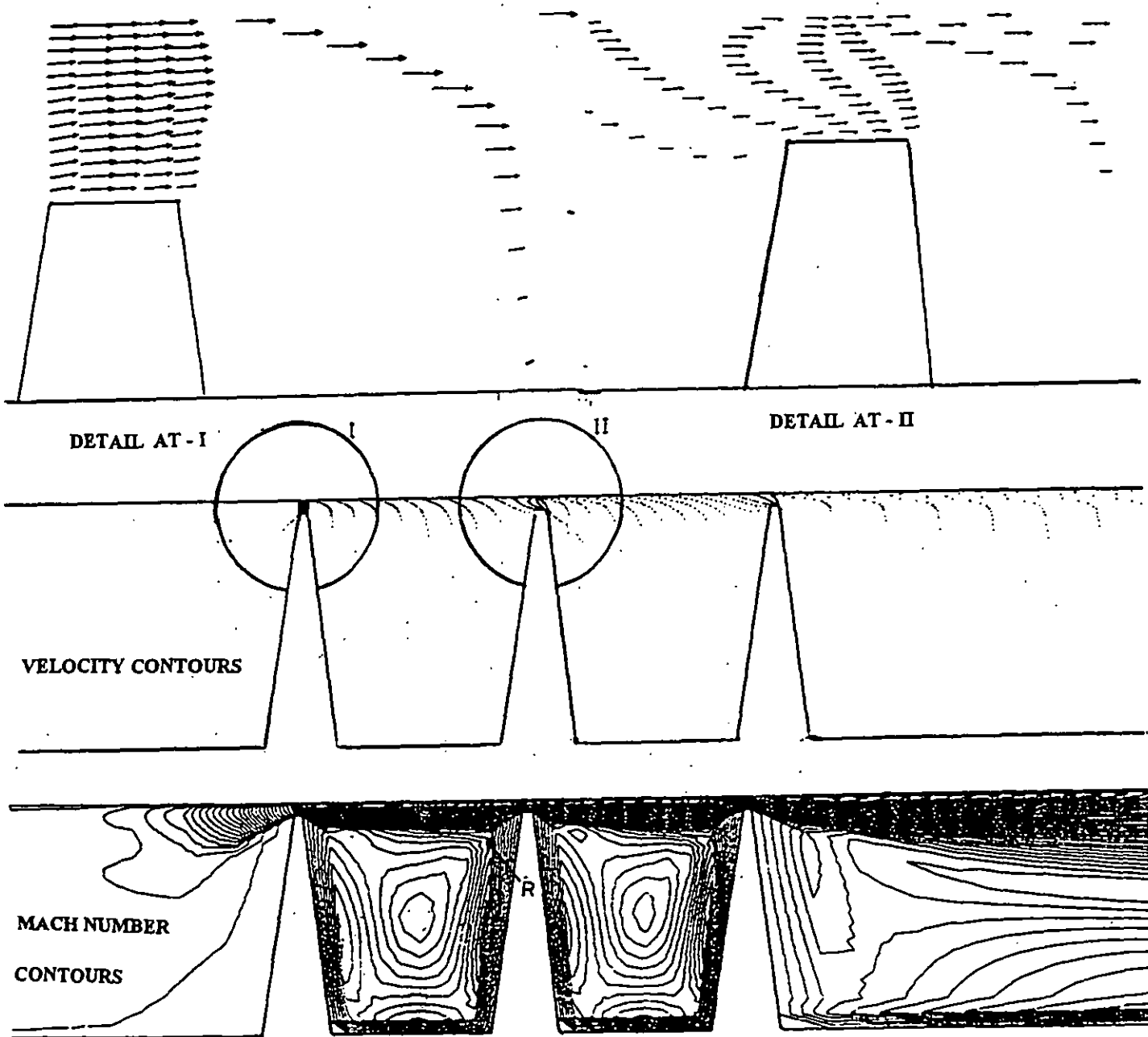


FIG. 3 VELOCITY VECTOR AND MACH NUMBER CONTOUR PLOTS FOR INCOMPRESSIBLE FLOW IN A STRAIGHT-THROUGH LABYRINTH SEAL ($p_0/p_1 = 1.89$)

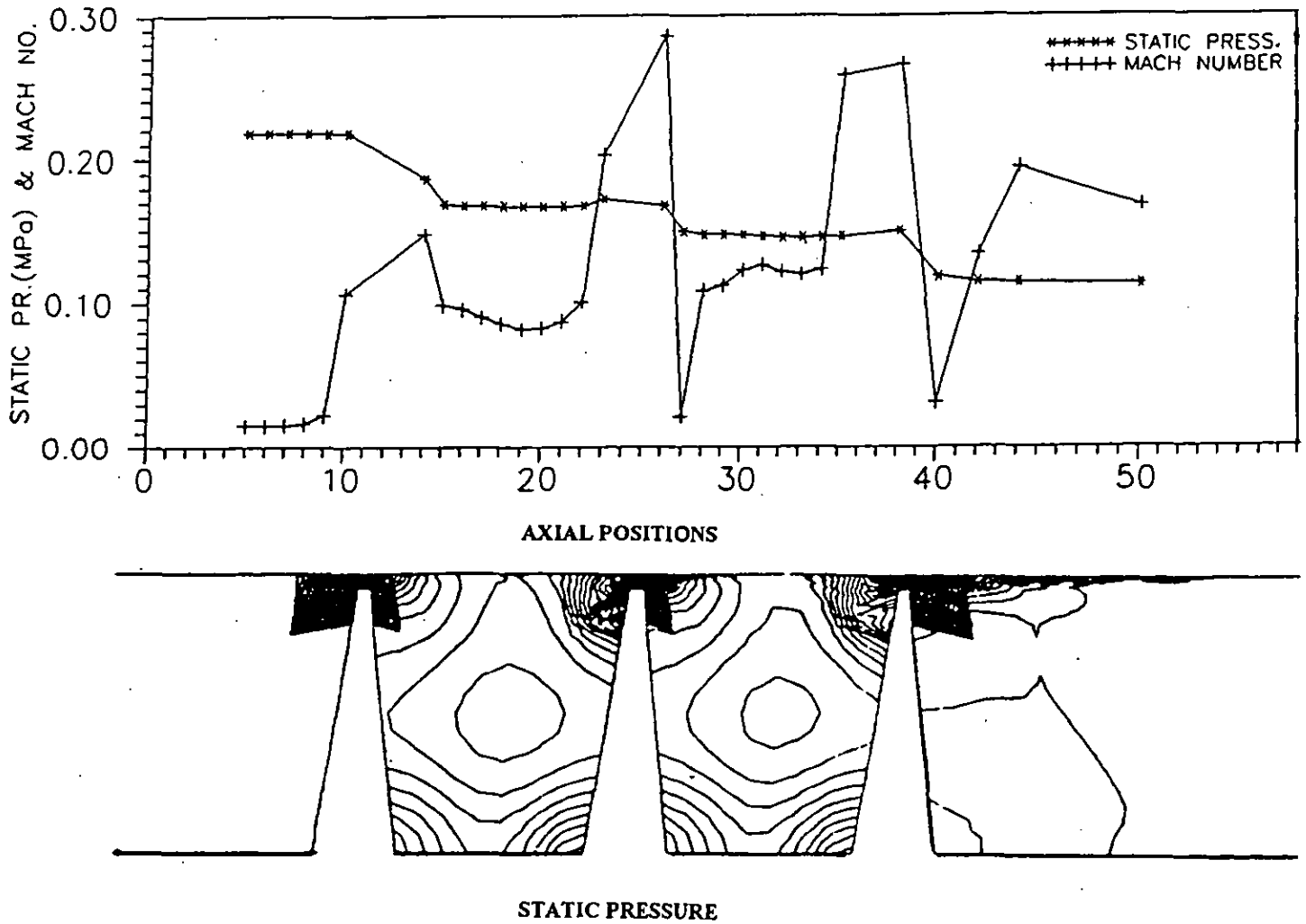


FIG.4 STATIC PRESSURE AND MACH NUMBER VARIATION FOR INCOMPRESSIBLE FLOW IN A STRAIGHT - THROUGH LABYRINTH SEAL ($p_0/p_1 = 1.89$)

Figure 5 shows the contours of the kinetic energy of turbulence. It is clear that the value of k increases as the flow passes through successive teeth. The increase in the turbulent kinetic energy also contributes to its dissipation rate and thereby to the pressure drop between the seal teeth and to resisting the leakage flow.

CONCLUSIONS:

Experiments were conducted, and the FLUENT computer code has been applied to determine the leakage flow from a typical straight-through labyrinth seal for a turbomachinery application. The integrated values of leakages flow rates, estimated from the computational results, agree with

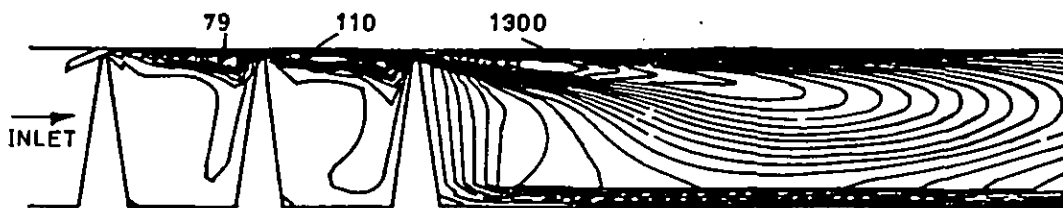


FIG. 5 KINETIC ENERGY OF TURBULENCE (M^2/Sec^2) ($p_0/p_1 = 1.89$)

the experimental data within 8.6%. The computational results are presented in the form of velocity and Mach number contours, static pressure variations and velocity vectors for the chosen seal geometry and pressure ratio. The features such as mean kinetic energy and static pressure variations in the successive seal cavities are shown. The behaviours of streamlines and Mach number contours are explained. The kinetic energy of turbulence is shown to be increasing from the first to the last seal cavity, thereby increasing the resistance to the flow leakage.

Acknowledgement:

The authors (VSM & NNR) wish to gratefully acknowledge the help and encouragement given to them by the Director, GTRE, Bangalore.

The authors acknowledge the computation facility provided to them by Dr. G. Venkata Rathnam of I.I.T., Madras. The authors wish to sincerely thank the reviewers for their suggestions to improve this paper.

REFERENCE

1. Stocker, H., 1978, "Determining labyrinth seal performance in current and advanced high performance gas turbines", Report No. AGARD-CP-237., Sec.13, pp.1-22.
2. Rhode, D.L. and Sobolik, S.R., 1986b, "Simulation of subsonic flow through a generic labyrinth seal, ASME Journal of Gas Turbine and Power, Vol.108, pp.674-679.
3. Martin, H.M., 1908, "Labyrinth Packings", Engineering, pp.35-36.
4. Egli, A., 1935, "The leakage of steam through Labyrinth seals", ASME Transactions, Vol.57, No.3., pp 115-122.
5. Kearton, W.J. and Keh, T.H. 1950, "Leakage of air through labyrinth glands of staggered type", Proc. I Mech. E., Vol.166, pp.180-195.
6. Vermes, G., 1961, "A fluid mechanics approach to the labyrinth seal problem", ASME Journal of Lubrication Technology, pp.161-169.
7. Koenig, H.A. and Bowley, W.W., 1972, "Labyrinth seal analysis", ASME Journal of Lubrication Technology, pp.5-11.
8. Mahler, F.H., 1972, "Advanced Seal Technology", Pratt & Whitney Aircraft, East Hartford, Connecticut, Feb, 1972, NTIS report no. AD 739 922 NTIS.
9. Fluid flow division, 1973, "Duct systems - Labyrinth seals", General Electric Review, Sec.405.7, pp.1-25.
10. Meyer, C.A. and Lowrie, J.A., 1975, "The leakage through and slant labyrinths and Honey comb seals, ASME Journal of Engineering for Power, pp.495-502.
11. Komotori, K. and Miyake, K., 1977, "Leakage characteristics of labyrinth seals with high rotating speed", Tokyo Joint Gas turbine Congress, pp.371-380.
12. Stoff, H., 1980, "Incompressible flow in a labyrinth seal", Journal of Fluid Mechanics, Vol.100, part 4, pp.817-829.
13. Rhode, D.L., Demko, J.A., Traegner, U.K., Morrison, G.L. and Sobolik, S.R., 1986 a, "Prediction of incompressible flow in labyrinth seals", Journal of Fluids Engineering", Vol.108, pp.19-25.
14. Sturgess, J.G. and Datta, P., 1988, "Application of CFD to gas turbine engine - Labyrinth seals", AIAA Report No.A88-44791, pp.1-12.
15. Brownell, J.B., Milward, J.A. and Parker, R.J., 1989, "Non-intrusive investigations into life-size labyrinth seal flow fields", ASME Journal of Engineering for Gas Turbines and Power, Vol.11, pp.335-342.
16. Demko, J.A., Morrison, G.L. and Rhode, D.L., 1990, "Effect of shaft rotation on the incompressible flow in a labyrinth seal", Journal of propulsion, Vol.6, pp.171-176.
17. Zhu Yizhang and He Feng, 1990, "Analysis of leakage characteristics of labyrinth seals, Chinese Journal of Aeronautics, Vol.3, No.4, pp.233-238.
18. Rhode, D.L. and Nail, G.H., 1992a "Computation of cavity-by-cavity flow development in generic labyrinth seals, ASME Journal of Tribology, Vol.114, pp.47-51.
19. Rhode, D.L. and Hibbs, R.I. 1992b, "Tooth thickness effect on the performance of gas labyrinth seals", ASME Journal of Tribology, Vol.114, pp.790-795.
20. Milward, J.A. and Edwards, M.F., 1996, "Windage heating of air passing through labyrinth seals", ASME Journal of Gas Turbine and Power, Vol.118, pp.414-419.
21. Sethu Manavalan, V. and Nanjunda Rao, N., 1989, "Experimental investigation of straight-through and inclined Labyrinth seals", Gas Turbine Research Establishment, India, Internal Technical Paper No.ZCS-002.
22. Sethu Manavalan, V. and Nanjunda Rao, N., 1992, "Effect of Rotation on Leakage flow characteristics of stepped labyrinth seals" Gas Turbine Research Establishment, India, Internal Technical Paper No.ZCS-004.
23. Sethu Manavalan, V. and Nanjunda Rao, N., 1996, "Performance characteristics of straight through and inclined labyrinth seals with Honeycomb lands, Gas Turbine Research Establishment, India Internal Technical Paper No.ZCS-003.
24. Sneek, H.J., 1974, "Labyrinth seal literature survey", ASME Journal of Lubrication Technology, pp.579-582.
25. Rhode, D.L., Broussard, D.H. and Veldanda, S.B., 1993a, "Labyrinth seal leakage resistance and visualization experiments in a novel, variable - configuration facility", Tribology Trans., Vol.36, 2, pp.213-218.
26. Rhode, D.L. and Guidry, M.J., 1993b "A new approach for stabilizing labyrinth seal leakage", Tribology Trans., Vol.36, 2, pp.219-224.
27. Rhode, D.L. and Guidry, M.J., 1993c, "Importance of labyrinth seal through-flow deflection for enlarging clearance without increasing leakage", Tribology Trans., Vol.36,3, pp.477-483.
28. Sethu Manavalan, V., 1997, "Analysis of flow through labyrinth seals in Gas turbines", M.Tech. Thesis, Mechanical Engineering Department, I.I.T., Madras, India.